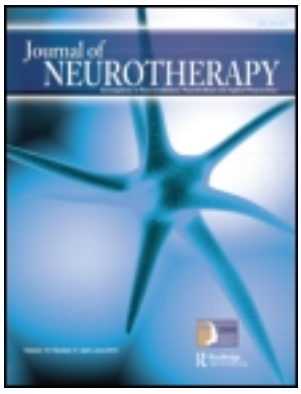

Journal of Neurotherapy: Investigations in Neuromodulation, Neurofeedback and Applied Neuroscience

Publication details, including instructions for authors and subscription information:
http://www.tandfonline.com/loi/wneu20

Latest Developments in Live Z-Score Training: Symptom Check List, Phase Reset, and Loreta Z-Score Biofeedback

Robert W. Thatcher PhD [a]

[a] EEG and NeuroImaging Laboratory, Applied Neuroscience Research Institute, St. Petersburg, Florida, USA

Published online: 26 Feb 2013.

To cite this article: Robert W. Thatcher PhD (2013): Latest Developments in Live Z-Score Training: Symptom Check List, Phase Reset, and Loreta Z-Score Biofeedback, Journal of Neurotherapy: Investigations in Neuromodulation, Neurofeedback and Applied Neuroscience, 17:1, 69-87

To link to this article: http://dx.doi.org/10.1080/10874208.2013.759032

Journal of Neurotherapy, 17:69–87, 2013

ISSN: 1087-4208 print/1530-017X online
DOI: 10.1080/10874208.2013.759032

Routledge
Taylor & Francis Group

LATEST DEVELOPMENTS IN LIVE *Z*-SCORE TRAINING: SYMPTOM CHECK LIST, PHASE RESET, AND LORETA *Z*-SCORE BIOFEEDBACK

Robert W. Thatcher

EEG and NeuroImaging Laboratory, Applied Neuroscience Research Institute, St. Petersburg, Florida, USA

Advances in neuroscience are applied to the clinical applications of EEG neurofeedback by linking symptoms to functional networks in the brain. This is achieved by reviews of the last 20 years of functional neuroimaging studies of brain networks related to clinical disorders based on positron emission tomography, functional MRI, diffusion tensor imaging, and EEG/MEG inverse solutions. Considerable consistency exists between different imaging modalities because of the property of functional localization and the existence of large clusters of connections in the brain representing network modules and hubs. Reviewed here is new method of EEG neurofeedback called *Z*-Score Neurofeedback, and it is demonstrated how real-time comparison to an age-matched population of healthy subjects simplifies protocol generation and allows clinicians to target modules and hubs that indicate dysregulation and instability in networks related to symptoms. *Z*-score neurofeedback, by measuring the distance from the center of the healthy age-matched population, increases specificity in operant conditioning and provides a guide by which extreme *Z*-score outliers are linked to symptoms and then reinforced toward states of greater homeostasis and stability. The goal is increased efficiency of information processing in brain networks related to the patient's symptoms. The unique advantage of EEG over other neuroimaging methods is high temporal resolution in which the fine temporal details of phase lock and phase shift between large masses of neurons is quantified and can be modified by *Z*-score neurofeedback to address the patient's symptoms. The latest developments in *Z*-score neurofeedback are a harbinger of a bright future for clinicians and, most important, patients that suffer from a variety of brain dysfunctions.

SPECIFICITY AND GOOD CLINICAL OUTCOME WITH FEWER SESSIONS

The last 60 years of EEG biofeedback have resulted in a wide range of biofeedback approaches, but many report good clinical outcomes only after 40 to 80 sessions. This includes evidenced-based medicine (EBM) studies using sham controls and/or blind designs that typically require 40 sessions or more to achieve a good clinical outcome (Arns, de Ridder, Strehl, Breteler, & Coenen, 2009; Wangler et al., 2011). The scientific reality of EEG biofeedback has been well established since the 1940s, as reviewed by Sherlin et al. (2011) and Thatcher (2012). However, the challenge today is to achieve good clinical outcomes in fewer than 40 to 80 sessions. An important fact is that real-time fMRI neurofeedback can achieve modification of blood flow in specific brain regions in one 20-min session (see Dr. Niels Birbaumer explain why only 20 min is required at the GoCognitive website; GoCognitive, n.d.-a, n.d.-b). The reason that a single 20-min session achieves clinical change is because of adherence to the principles of specificity and contingency in operant conditioning (Balleine & Dickinson, 1998; Balleine, Liljeholm, & Ostlund, 2009; Balleine

Received 6 September 2012; accepted 29 November 2012.
Address correspondence to Robert W. Thatcher, PhD, EEG and NeuroImaging Laboratory, Applied Neuroscience Research Institute, 228 176th Terrace Drive, St. Petersburg, FL 33708, USA. E-mail: rwthatcher2@yahoo.com

& Ostlund; 2007; Schultz, 2006). For example, the fMRI neurofeedback method targets a single Brodmann area of the brain linked to the patient's symptoms. In contrast, surface EEG is diffuse and less specific; for example, the EEG recorded from a single scalp location (e.g., Cz) senses sources from widespread regions of the brain and is a mixture of many different frequencies. Use of surface *Z* scores improves specificity by isolating dysregulated locations and rhythms, especially when using Laplacian transformed *Z* scores. Comparable specification and localization, as in fMRI, is achieved by LORETA *Z*-score neurofeedback. For example, clinical experience suggests that LORETA *Z*-score neurofeedback often produces results in one 20-min session like fMRI neurofeedback because EEG source localization has accuracies of about 1 cm to 3 cm and thus is much more specific than is surface EEG (see Applied Neuroscience, n.d.). Hence, targeting specific ''hubs'' and ''modules'' linked to a patient's symptoms seems to result in good clinical outcomes in fewer sessions than does surface EEG biofeedback (see Thatcher, 2012).

As mentioned previously, the goal of *Z*-score biofeedback is to achieve improved clinical outcome in fewer sessions. The *Z*-score approach is more efficient because it is based on a quantitative EEG (qEEG) assessment in which a patient's symptoms and complaints are linked to functional systems in the brain to identify the ''weak'' systems, as defined by Luria (1973), and then targets the weak systems for neurofeedback in the same session. Increased specificity also includes not modifying ''compensatory'' systems and thereby improves the efficiency of EEG biofeedback (i.e., fewer sessions with equal or better clinical outcomes in comparison to non-*Z*-score biofeedback). Since 2006 there have been a few publications showing good clinical outcomes with 20 or fewer

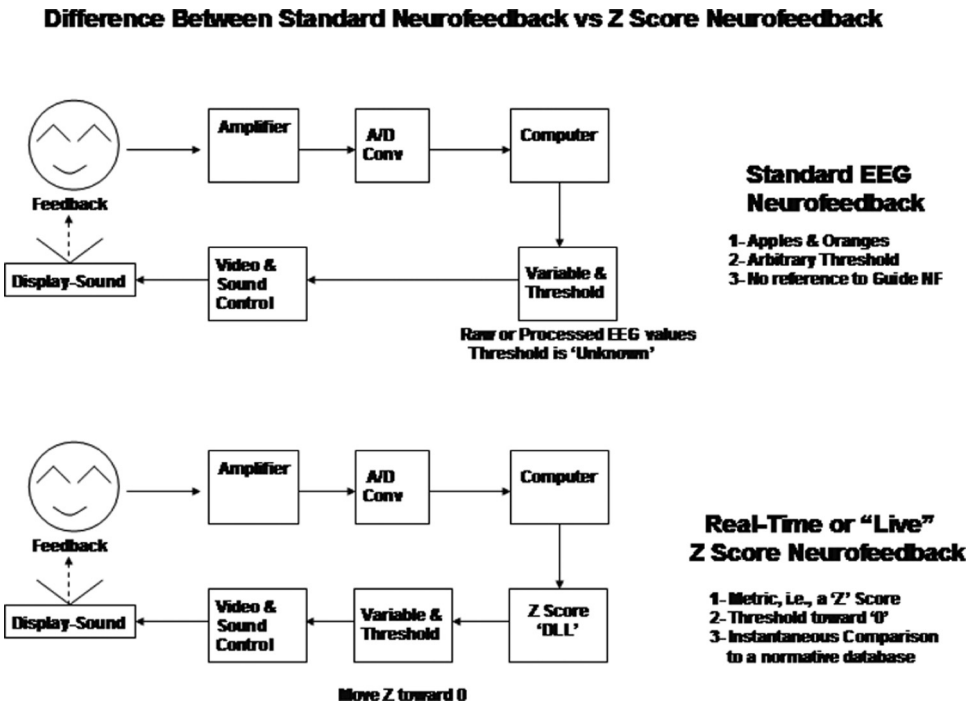

FIGURE 1. Top row is conventional or standard EEG biofeedback in which different units of measurement are used in an EEG analysis (e.g., uV for amplitude, theta/beta ratios, relative power 0 to 100%, coherence 0 to 1, phase in degrees or radians, etc.) and the clinician must ''guess'' at a threshold for a particular electrode location, frequency range and client age to determine when to reinforce or inhibit a given measure. The bottom row is *Z*-score neuofeedback in which different metrics are represented by a single and common metric (i.e., the metric of a *Z* score), and the guess work is removed because all measures are reinforced to move *Z* scores toward $Z = 0$, which is the approximate center of an average healthy brain state based on a reference age-matched normative database in real time.

sessions using *Z*-score neuroeedback, and several new publications are in process (Collura, Guan, Tarrant, Bailey, & Starr, 2010; Hammer, Colbert, Brown, & Ilioi, 2011). Figure 1 illustrates the difference between conventional EEG neurofeedback versus *Z*-score neurofeedback.

Z-SCORE BIOFEEDBACK—OUTLIERS AND MINIMIZATION OF UNSTABLE AND INEFFICIENT NETWORKS

QEEG normative databases are constructed and validated by using scientific standards such as sufficient sample size per age group, Gaussianity, clear inclusion/exclusion criteria, no artifact, cross-validation, amplifier matching, and peer-reviewed publications (John, Prichep, & Easton, 1987; Thatcher & Lubar, 2008; Thatcher, North, & Biver, 2008a). On the average, approximately 95% of healthy normal subjects exhibit EEG values that are within 2 *SD*s of the mean of the population and 98.7% are within 3 *SD*s. Normative databases provide a representative sampling of healthy individuals including high-functioning children and adults. Comparison to a normal reference population aids in identifying outliers or extreme scores that may help the clinician to link symptoms to dysregulation in the brain. Rarely is just one electrode or one measure deviant from normal; instead, deviations from normal, when linked to symptoms, often occur in clusters of measures related to networks. However, clinicians are cautioned to use only normative references to aid in the evaluation of patients with symptoms and not peak performance individuals who may exhibit extreme scores unrelated to a clinical problem. Also, clinicians must be careful not to use a *Z*-score normative database that fails to match amplifier characteristics and/or fails to disclose the details of the database (see Thatcher & Lubar, 2008).

A recent example of a new application of a normative database is the use of complex demodulation as a *Z*-score Joint-Time-Frequency-Analysis (JTFA) for the purposes of real-time neurofeedback (Thatcher, 1998, 1999, 2000a, 2000b). The *Z* score is computed in microseconds, limited by the sample rate of the EEG amplifier, and therefore are ''instantaneous'' *Z* scores. It is necessary under the principles of operant conditioning that contiguity not be too fast because the activation of dopamine and other neuromodulators is relatively slow and long-lasting. Therefore, a time interval of 250 ms to a few seconds between the detection of a brain event meeting threshold and the delivery of a reinforcement or the contiguity interval is commonly used in standard EEG biofeedback that does not involve *Z* scores.

In 2006, the real-time *Z*-score biofeedback method was implemented by Brainmaster, Inc. and by Thought Technology, LLC, and later by Mind Media, Inc.; Deymed, Inc.; and EEG Spectrum, Inc., as well as Applied Neuroscience, Inc. Since 2006, more than 1,200 clinicians have been using *Z*-score EEG neurofeedback. All implementations of ''Live *Z* Score'' biofeedback, also called ''real-time *Z* score'' neurofeedback, share the goal of using standard operant learning methods to modify synapses in brain networks, specifically networks modified by long-term potentiation (LTP) and N-Methyl-D-Aspartate receptors as illustrated in Figure 2. Operant conditioning is known to involve changes in the same N-Methyl-D-Aspartate receptors that are modified in LTP; therefore, the unifying purpose of *Z*-score biofeedback is to reinforce extreme scores or outliers toward $Z = 0$ of the EEG which is the statistical ''center'' or set-point of a group of healthy normal subjects. The normal subjects are a reference, as with blood tests for cholesterol or liver enzymes showing deviation from normal that serve as indicators to the clinician who tests hypotheses and uses multiple tests to derive a diagnosis and select treatments.

UNIFIED PRINCIPLE OF Z-SCORE BIOFEEDBACK

All *Z*-score biofeedback methods are unified by the goal of modifying outlier *Z*-scores generated by the brain toward greater homeostasis and

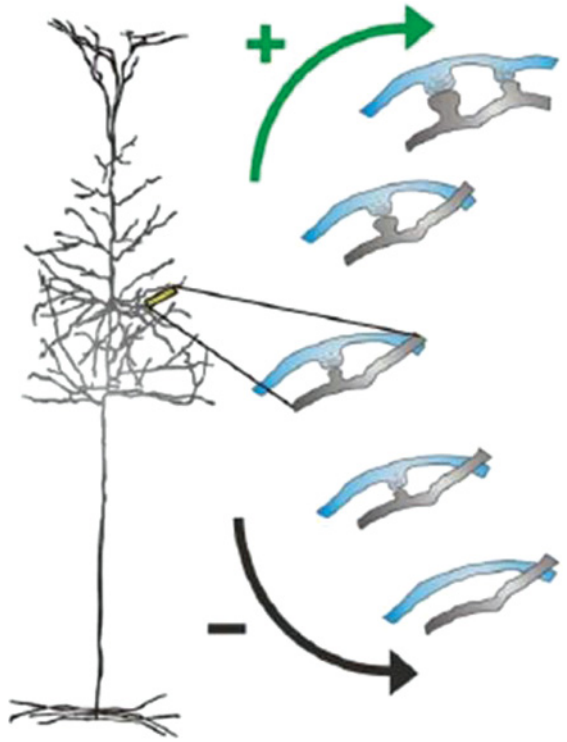

FIGURE 2. Illustration of long-term potentiation (+) and long-term depression (–). Operant conditioning involves modification of synapses by the action of neuromodulators such as dopamine, seratonin, acetylcholine, and so on. (From Ed Pigot based on Kandel, 2006; Nargeot, Baxter, & Byrne, 1999; Nargeot, Baxter, Patterson, & Byrne, 1999.) (Color figure available online.)

fewer extreme and unstable states. *Z*-score biofeedback has its greatest impact on unstable or dysregulated neural systems because only small *Z*-score values are reinforced and unstable systems that produce extreme *Z* scores are reinforced by the operant or instrumental learning procedure only when the scores move in the direction of $Z = 0$. The center of the normal population or the ideal instantaneous $Z = 0$ is only a statistical ideal in which homestatic and balanced systems oscillate around, but never achieve, perfect $Z = 0$ for the entire system or subsystems. However, on average, unstable neural states that produce large *Z*-score values (e.g., 5 *SD*s or 3 *SD*s, etc.) will be minimized and stable neural states that are less than 2 standard deviations will be reinforced. This is the same process that occurs at a slower speed with blood tests; for example, a blood test that shows low blood iron results in ingestion of iron pills that increases blood iron toward $Z = 0$, which is the mean of the reference normal population. In the case of *Z*-score neurofeedback, the duration and frequency of unstable states or periods of dysregulation that are 2 or more standard deviations are identified to aid linkage of the ''outliers'' or extreme neural network EEG values to symptoms and then to construct a protocol to target the mostly likely dysregulated modules and hubs by reinforcing the extreme outliers in the EEG toward $Z = 0$. In other words, the reference normative database provides a method to identify outliers linked to symptoms while providing a real-time direction toward increased stability in networks of the brain linked to those symptoms.

Complex demodulation is an analytic technique that multiplies a time series by a sine wave and a cosine wave and then applies a low pass filter (Granger & Hatanka, 1964; Otnes & Enochson, 1978). This results in mapping of the time series to the unit circle or complex plane, whereby instantaneous power and instantaneous phase differences and coherence are computed. Figure 3 is an illustration of complex demodulation to compute instantaneous power, coherence, and phase differences.

Unlike the Fourier transform, which depends on windowing and integration over an interval of time, complex demodulation computes the instantaneous power and phase at each time point, and thus an instantaneous *Z* score necessarily includes the within-subject variance of instantaneous electrical activity as well as the between-subject variance for subjects of a given age. The summation of instantaneous *Z* scores is Gaussian-distributed and has high cross-validation (Thatcher, North, & Biver, 2005; Thatcher, Walker, Biver, North, & Curtin, 2003); however, the individual time point by time point *Z* score is always smaller than the summation due to within subject variance. The use of within subject variance results in a more ''conservative'' estimate of deviation from normal solely for the purposes of instantaneous neurofeedback methods. Figure 4 illustrates the difference between the ''live *Z* Score'' (JTFA) versus Fast Fourier Transform (FFT) *Z*-score computations.

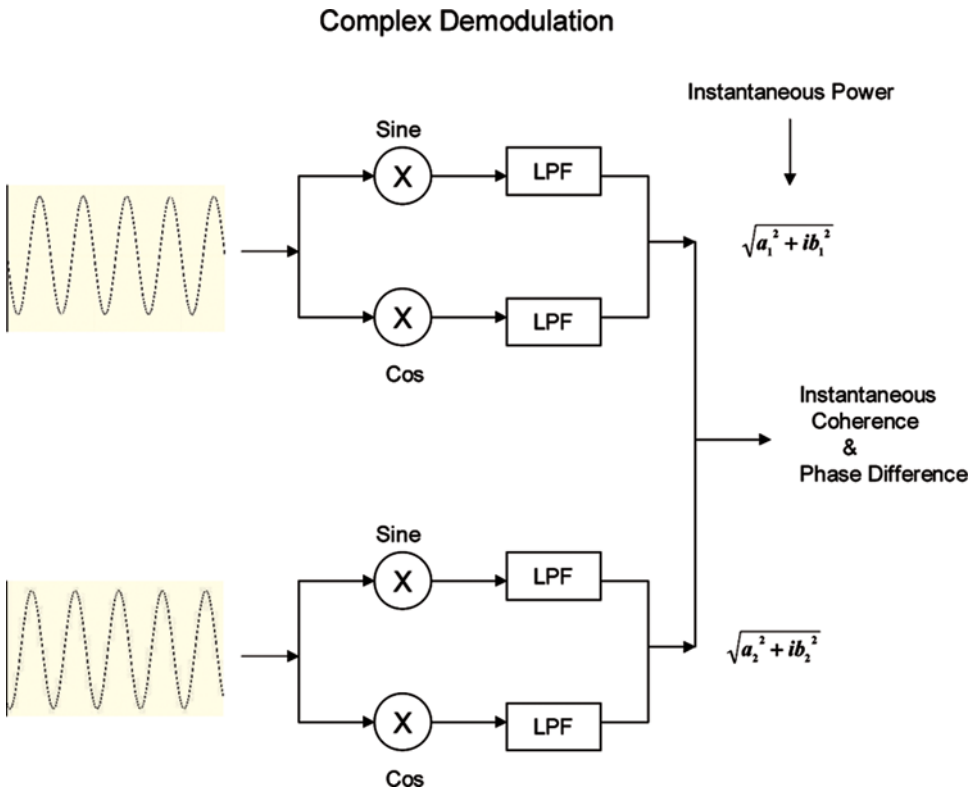

FIGURE 3. Illustration of complex demodulation to compute *Z* scores at each time sample. Left is a sine wave input that is multiplied by the sine and cosine waves at the center frequency of a given frequency band, which transforms the digital time series to the complex plane. A 6th order Butterworth low-pass filter is used to shift the frequency to zero where power at the center frequency is then calculated using the Pythagorean theorem. Complex numbers are then used to compute coherence and phase differences between two time series. (Color figure available online.)

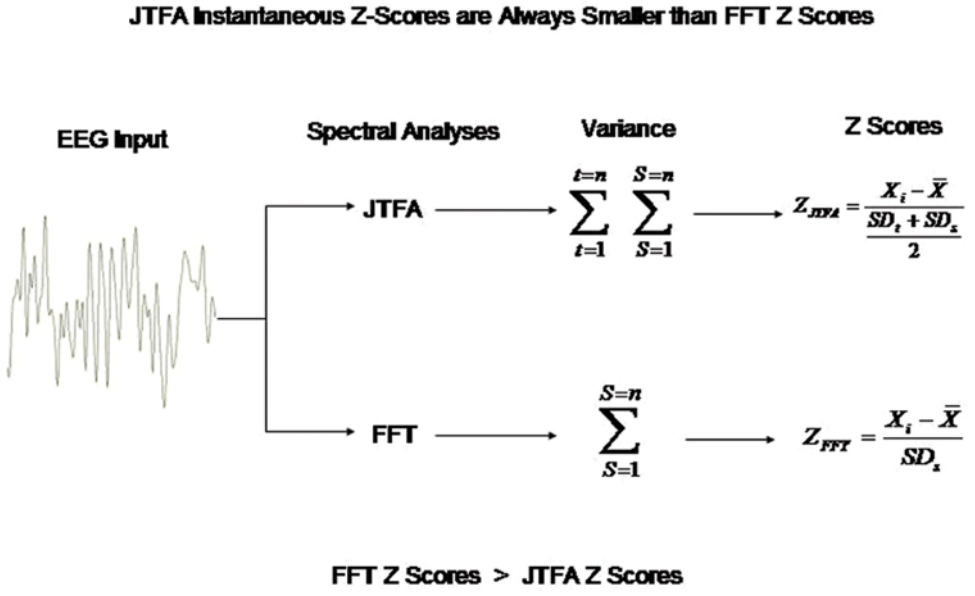

FIGURE 4. Joint-Time-Frequency-Analysis (JTFA) normative databases are instantaneous and include within session variance plus between subject variance. In contrast, Fast Fourier Transform (FFT) normative data only contains between subject variance. Thus FFT *Z* scores are larger than JTFA *Z* scores; and a ratio of 2:1 is not uncommon. *Note*. t = time; s = subjects; *SD*t = standard deviation for the within session; *SD*s = standard deviation between subjects. (Color figure available online.)

A standard FFT normative database analysis should first be computed to identify the electrode locations and EEG features that are most deviant from normal and that can be linked to the patient's symptoms and complaints. Linking a subject's symptoms and complaints (e.g., posttraumatic stress disorder, depression, schizophrenia, traumatic brain injury, etc.) to functional localization of the brain is an important objective of those who use a normative database. Linking dysregulation of neural activity or extreme *Z* scores in modules and hubs of the brain known to be related to function are important facts in the hands of a trained clinician. Textbooks on functional localization in neurology and psychiatry are available to aid the clinician in learning about the link between a patient's symptoms and different brain regions (Clark, Boutros, & Mendez, 2010; Luria, 1973; Mesulam, 2000; Tonkonogy & Puente, 2009). A link of the anatomical locations and patterns of a patient's extreme *Z* scores is important in order to derive clinical meaning from the qEEG.

Once a qEEG normative database analysis is completed, then one can use a *Z*-score neurofeedback program to train patients to move outlier *Z* scores toward zero or toward the center of the age-matched normal population. The absolute value and range of the instantaneous *Z* scores, although smaller than those obtained using the offline qEEG normative database, are simply scaled to smaller values and are valid and capable of being reinforced toward zero. An advantage of a *Z*-score neurofeedback program is simplification by reducing diverse measures like power, ratios, coherence, or phase to a single metric (i.e., the metric of a *Z* score). Thus, there is greater standardization and less guesswork about whether to reinforce or suppress coherence or phase differences or power and so forth at a particular location and particular frequency band. The difference between standard or conventional EEG neurofeedback versus *Z*-score neurofeedback is shown in Figure 1.

Figure 5 shows the number of subjects per year in the *Z*-Score normative EEG database

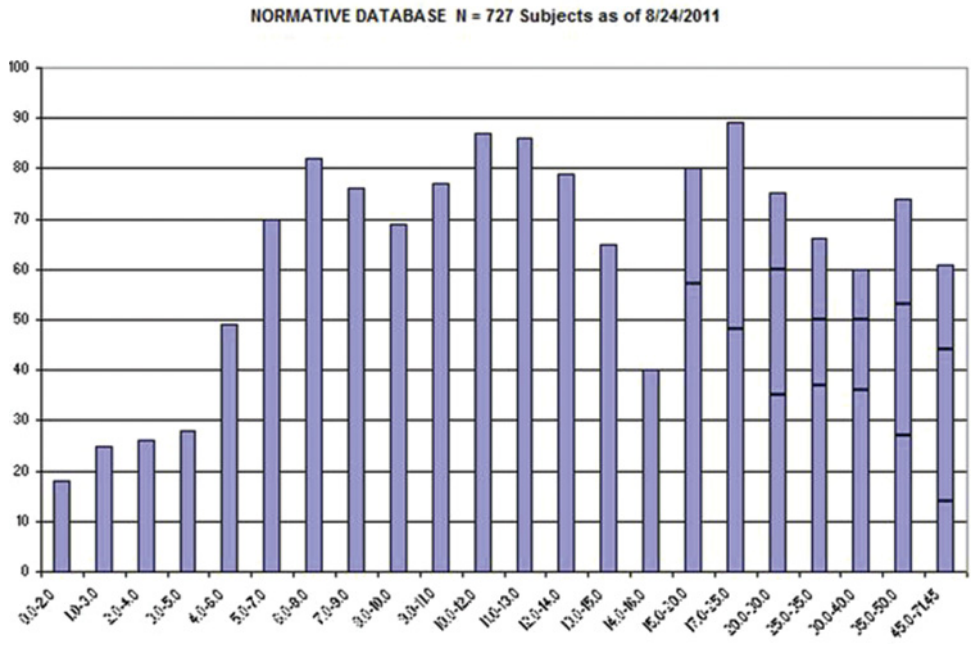

FIGURE 5. The number of subjects per age group in the *Z* score Lifespan EEG reference normative database. The database is a ''life-span'' database with 2 months of age being the youngest subject and 82.3 years of age being the oldest subject. Two-year means were computed using a sliding average with 6-month overlap of subjects. This produced a more stable and higher age resolution normative database and a total of 21 different age groups. The 21 age groups and age ranges, and the number of subjects per age group are shown in the bar graph. (Color figure available online.)

($N = 727$) that spans the age range from 2 months to 82 years of age. It can be seen that the largest number of subjects are in the younger ages (e.g., 1–14 years, $n = 470$) when the EEG is changing most rapidly. A proportionately smaller number of subjects represents the adult age range from 14 to 82 years ($n = 155$). To increase the time resolution of age, sliding averages were used for age stratification of the instantaneous *Z* scores for purposes of EEG biofeedback. Two-year means were computed using a sliding average with 6-month overlap of subjects. This produced a more stable and higher age resolution normative database and a total of 21 different age groups. The 21 age groups and age ranges, and the number of subjects per age group, are shown in the bar graph in Figure 5.

PHASE RESET AND EEG BIOFEEDBACK

Phase reset (PR) is a process defined by a phase shift followed by phase lock, which generates ordered sequences of metastable states as a core component of information flow in the brain. Multielectrode recordings and EEG experiments indicate that brain information dynamics are a sequence of controllable instabilities (Breakspear & Williams, 2004; Freeman, Homes, West, & Vanhatlo, 2006; John, 2005; Rabinovich, Afraimovich, Christian, & Varona, 2012; Stam & van Straaten, 2012; Thatcher, North, & Biver, 2008b, 2009; Varela, 1995). PR occurs in coupled nonlinear oscillators when there is a sudden phase shift between oscillators to a new value followed by a period of phase locking or phase stability, also called phase synchrony (Pikovsky, Rosenblum, & Kurths, 2003). The term *phase synchrony* is synonymous with phase locking; and whether one refers to phase locking or phase synchrony, what is important is the fact that there is a prolonged period of phase stability following a phase shift (Tass, 2007). PR is also important because it results in increased EEG amplitudes due to increased phase synchrony of synaptic generators (Cooper, Winter, Crow, & Walter, 1965; Hughes & Curnelli, 2007; Lopes da Silva, 1995; Nunez, 1981, 1995).

JTFA must trade off frequency resolution for time resolution and vice versa. The complex demodulation computation is over a frequency range such as the EEG delta, theta, alpha, and beta frequency ranges in order to increase the degrees of freedom in the computation of coherence. Given today's computers, less than a microsecond is needed to calculate the sample time point by sample time point of phase differences that forms a new EEG time series of phase differences between pairs of channels. If the instantaneous phase difference between two time series is constant, then the first derivative of phase differences will approximate zero and is called phase lock. A significant positive or negative first derivative of the time series of instantaneous phase differences represents a phase shift and marks the onset of phase locking.

Phase shift is defined by a change in phase differences, whereas phase lock is defined by no change in the phase difference between two oscillators over time. Mathematically, phase lock is defined as the first derivative equals zero or at least approximates zero within some reasonable bound. If there is a sudden change in phase difference (i.e., large first derivative), then this is the beginning of a phase shift. Figure 6 illustrates the concept of phase reset. Coherence is a measure of phase consistency or phase clustering on the unit circle as measured by the length of the unit vector *r*. The illustration in Figure 6 shows that the resultant vector $r_1 = r_2$; therefore, coherence, when averaged over time, is constant even though there can be a shift in the phase angle (i.e., phase difference) that occurs during the summation and average of the computation of coherence. This illustrates the advantage of phase differences that are ''instantaneous'' because computation is at temporal resolution of the sample rate and is not a statistical average like coherence and a correlation coefficient. This is important because time domain measures can be correlated with physiological events such as excitatory and inhibitory postsynaptic potential (i.e., IPSP and EPSP) durations. Details for computing complex demodulation and instantaneous spectra are described by Thatcher et al. (2008b) and Thatcher, North, Neurbrander, et al. (2009).

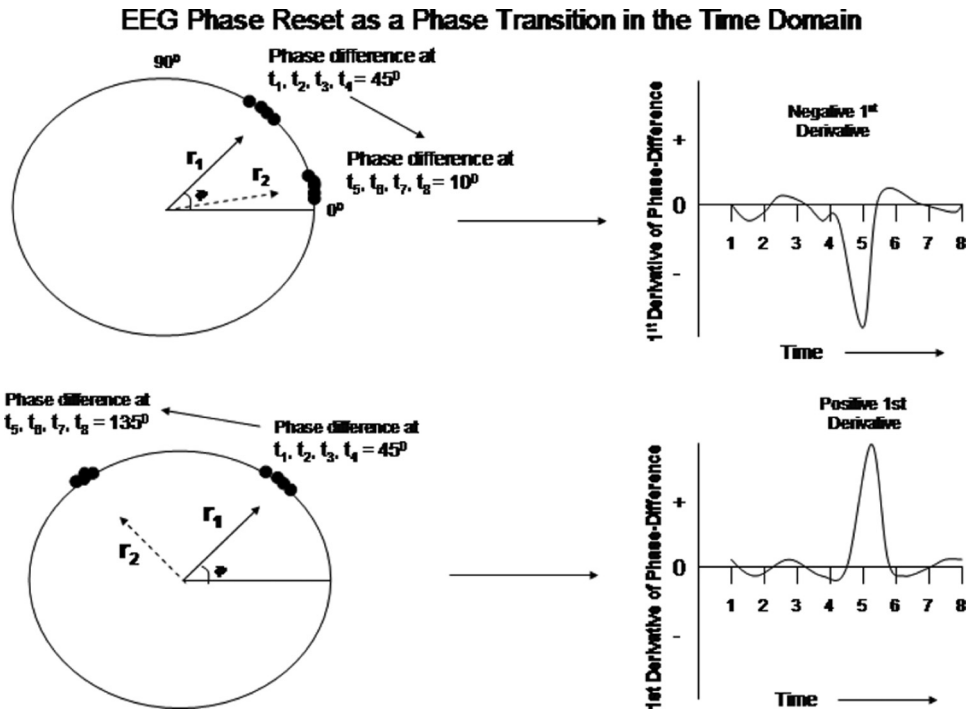

FIGURE 6. Illustrations of phase reset. Left is the unit circle in which there is a clustering of phase angles and thus high coherence as measured by the length of the unit vector *r*. The vector $r_1 = 45°$ occurs first in time and the vector $r_2 = 10°$ and 135° occurs later in time. The transition is between time point 4 and 5 where the first derivative is a maximum. The right displays are a time series of the approximated first derivative of the instantaneous phase differences for the time series t_1, t_2, t_3, t_4 at mean phase angle = 45° and t_5,t_6,t_7, t_8 at mean phase angle = 10°. Phase reset is defined as a significant negative or positive first derivative ($y' < 0$ or $y' > 0$). The first derivative near zero is when there is phase locking or phase stability and little change over time. The sign or direction of phase reset is arbitrary since two oscillating events are being brought into phase synchrony and represent a stable state as measured by EEG coherence independent of direction. The clustering of stable phase relationships over long periods of time is more common than are the phase transitions. The phase transitions are time markers of the thalamo-cortical-limbic-reticular circuits of the brain. (From Thatcher et al., 2008b.)

Recently, Stam and van Straaten (2012) reviewed some of the most common phase synchrony or phase lock measures used today. They pointed out that the Hilbert transform and wavelet transform are equivalent and the most commonly used measures in qEEG. A second set of measures are based on nonlinear dynamics that provide generalized synchronization estimates. A relatively simple unbiased estimator of generalized synchronization was developed by Stam and van Dijk (2002) and Montez, Linkenkaer-Hansen, Van Dijk, and Stam (2006). However, a limitation of these types of measures are that they provide only an estimate of the degree or average amount of synchrony between two time series and no information about the temporal duration of phase lock. Also, these measures fail to detect phase shift and do not provide temporal measures of phase shift duration. Phase shift and phase lock duration in the time domain are similar to the time domain of physiological events such as synaptic excitatory and inhibitory synaptic potentials (EPSPs and IPSPs) in large groups of subjects. An abstract measure of synchronization is interesting; however, the ability to relate synaptic potential durations to EEG phase lock and phase shift durations provides a more precise and dynamic measure of information processing. This is why there is emphasis on the use of complex demodulation and the Hilbert transform to provide accurate estimates of phase lock and phase shift duration with millisecond time resolution.

In general, the magnitude of phase shift is defined as the difference between the prephase shift value minus the postphase shift value; if a sudden and significant phase difference occurs

followed by an extended period of phase stability, then the point in time when the phase shift started is the time when the first derivative exceeded some threshold value (Breakspear & Williams, 2004; Le Van Quyen et al., 2001; Rudrauf et al., 2006; Tass, 2007). This point in time marks the onset of phase reset. EEG phase shift offset is defined in a reverse manner, and the onset and offset times define the phase shift duration. The phase shift duration is typically in the range of 30 ms to 80 ms (Buzaski, 2006; Freeman, Burke, & Homes, 2003; Freeman & Rogers, 2002). Phase locking or phase stability that follows a phase shift is often 200 ms to 600 ms in duration in single cell analyses (Gray, Konig, Engel, & Singer, 1989) and 200 ms to 1 s in surface recordings (Breakspear & Williams, 2004; Freeman et al., 2006; Freeman & Rogers, 2002). Desynchronization is the opposite of synchronization and is defined as a shift in the phase difference of synchronized oscillators and termination of phase locking. Notice in Figure 6 that both synchronization and desynchronization start with a phase shift or adjustment but differ in the sequential order. Figure 7 is an example of EEG phase reset as computed by the methods described in Figure 6.

Phase locking is a telltale sign of synchronization, and this is why Freeman and colleagues (Freeman et al., 2003; Freeman & Rogers, 2002) and Breakspear and Williams (2004) and others (Lachaux et al., 2000; Lachaux, Rodriguez, Martinerie, & Varela, 1999; LeVan Quyen et al., 2001; Varela, Lachaux, Rodriguez, & Martinerie, 2001) use phase locking as a measure of EEG synchronization. Of importance, neurons rapidly synchronize and the spatial extent of global or macro function is about 1 cm to 6 cm using fMRI, PET, EEG/MEG, multiple unit recordings, and other imaging modalities. This indicates that synchronization of large groups of pyramidal neurons is itself a fundamental property of information processing in the human brain.

Figure 8 is an example of filtered theta rhythms in the top screen and phase shift and

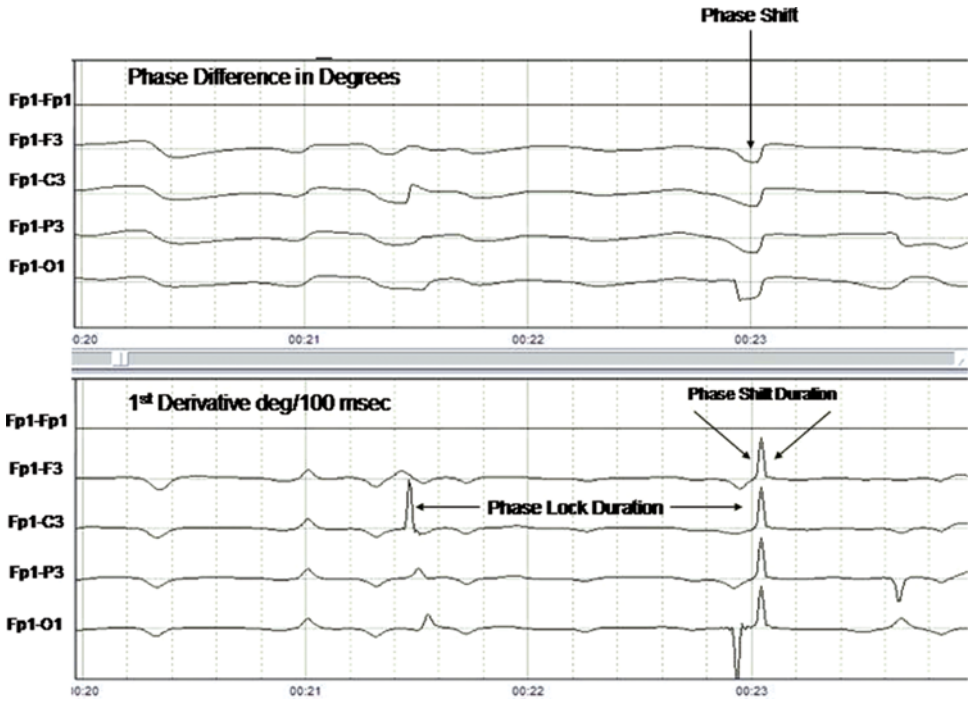

FIGURE 7. Example from one subject. Top are the EEG phase differences between Fp1-F3, Fp1-C3, Fp1-P3, and Fp1-O1 in degrees. Bottom are the first derivatives of the phase differences in the top traces in degrees/centiseconds. A first derivative $\geq 5°$/cs marked the onset of a phase shift and an interval of time following the phase shift where the first derivative ≈ 0 defined the phase synchrony interval as described in Figure 6. (Color figure available online.)

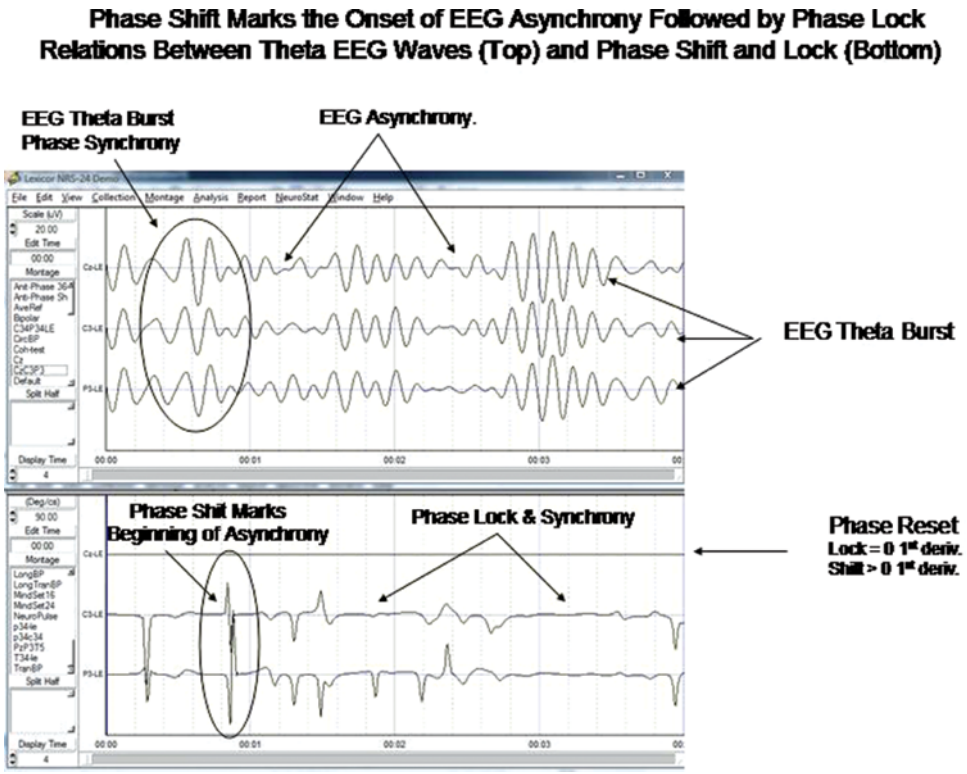

FIGURE 8. Top are filtered EEG traces in the theta frequency band (4–7 Hz) from Cz, C3 and P3, referenced to linked ears. Bottom is the first derivative of phase differences between the Cz time series and the time series from the other two electrodes. When the first derivative of phase differences are flat or approximate zero then this is an example of phase lock. The spikes or sudden change in the first derivative is a phase shift. Note that phase lock is associated with the high amplitude bursts of theta rhythms in the Top frame and the reduced amplitude or desynchronized periods are associated with phase shift. (From Thatcher, 2012.) (Color figure available online.)

phase lock in the bottom screen. Changes in large amplitude theta rhythms are marked by a spike in the first derivative of phase differences, which is a phase shift. Phase lock is dominant during rhythmic EEG bursts, and the transition between large amplitude synchrony and desynchrony is marked by a phase shift. Therefore, there is a direct correspondence between shifts and durations of rhythmic waves in the surface EEG and underlying phase shift and phase lock.

LORETA AND COUPLING OF MODULES AND HUBS

Another important fact is that the axonal connections of the human cortex are arranged in approximately six basic clusters, referred to as ''Modules,'' as measured by Diffusion Imaging Spectroscopy (Hagmann et al., 2008). Recently, the six fundamental modules measured by MRI Diffusion Imaging were replicated using qEEG Low Resolution Electromagnetic Tomography (LORETA; Thatcher, North, & Biver, 2012). LORETA is a distributed inverse solution of the three-dimensional sources of the surface recorded EEG (see Pascual-Marqui, Michel, & Lehmann, 1994, for details). Figure 9 shows LORETA locations of the replicated MRI Diffusion Imaging modules in Hagmann et al. (2008). Seventy-one of 71 subjects showed the same anatomical clustering for Modules 5 and 6, and 70 of 71 subjects showed the same modular structure for Module 1 (see Thatcher et al., 2012, for details).

The synaptic density of connections is spatially heterogeneous and clustered with phase shift and phase lock between clusters or Modules providing the ''vitality'' or temporal dynamics of the qEEG as determined in highly stable loops in thalamo-cortical, cortico-thalamic, and cortico-cortical connections. Pacemakers and natural resonance of pyramidal neurons and

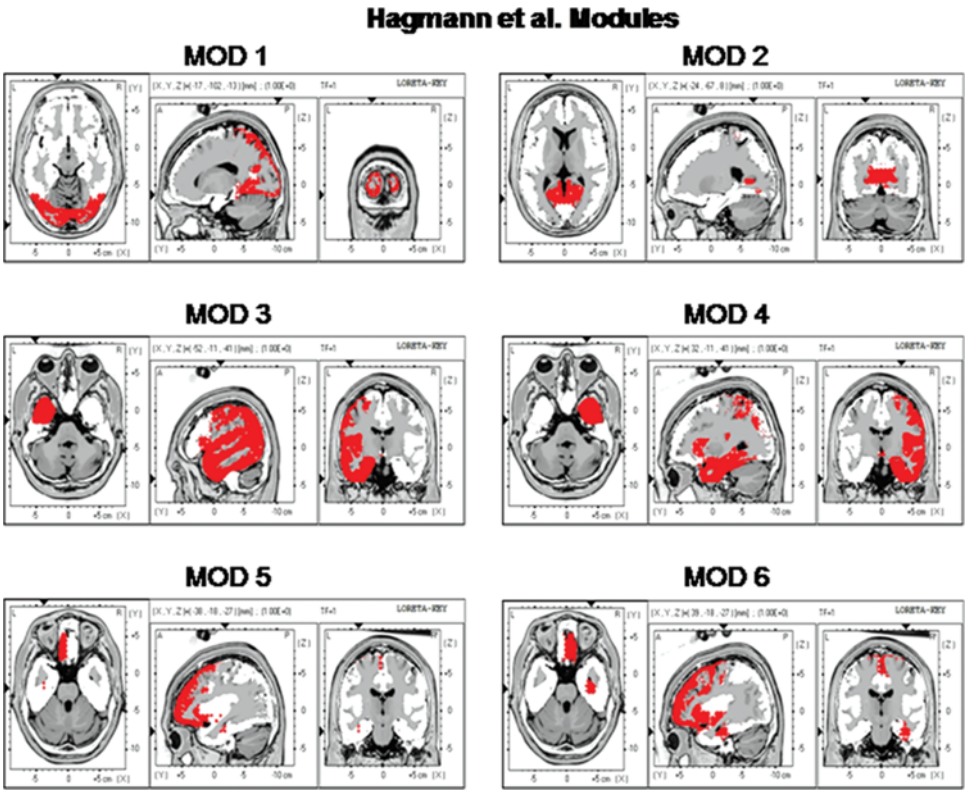

FIGURE 9. The locations of the six Hagmann et al. (2008) Modules as represented by the Key Institute LORETA voxels (Lancaster et al., 2000; Pascual-Marqui et al., 2004). As per Hagmann et al. (2008), Modules 3 and 4 are the same, but from different hemispheres. (Color figure available online.)

loops give rise to stable rhythms that operate like a ''Carrier Wave'' in which phase shift of neurons to ''In-Phase'' with respect to the local field potential are orchestrated by phase shift and phase lock mechanisms that are easily measurable in real time by standard quantitative qEEG methods (Buzsaki, 2006; Freeman et al., 2006; Varela, 1995; Wang, 2002). Distant excitatory synchronous inputs to functionally localized and specialized pyramidal neurons shifts frequency and the phase differences between different specialized brain regions over a period of approximately 30 ms to 80 ms (Thatcher et al., 2009). A large number of inhibitory interneurons are then excited and hyperpolarize large numbers of pyramidal neurons for a prolonged period (e.g., 100 ms to 800 ms), which is correlated with EEG phase lock duration across large-scale modules. Mathematical neural network models to simulate EEG phase shift and phase lock as well as memory based processes such as LTP and long-term suppression designate the initiator event at T = 0 to be synchronous with the arrival of long-distance excitatory inputs suddenly impinging on small specialized groups of neurons (i.e., local vs. distant network dynamics). It is the sudden arrival of excitatory synaptic inputs on the dendrites of pyramidal neurons that initiates the 10 ms to 80 ms phase shift followed by phase lock (Ermentrout, Galán, & Urban, 2007; Galán, Ermentrout, & Urban, 2005; Smeal, Ermentrout, & White, 2010; Tiesinga & Sejnowski, 2010). These three main models share the postulate that phase shift is initiated by distant excitatory inputs (i.e., cortico-cortical, thalamocortical, cortico-thalamic) onto local pyramidal neurons reaching maximum in, approximtely, a 40- to 80-msec interval of time. Phase shift is immediately followed by phase lock, which is mediated by a massive synchronous hyperpolarzied of pyramidal neurons via recurrent inhibition. Tiesinga and Sejnowski (2010) showed that large-scale and prolonged changes in

membrane potential of millions of neurons increases the probability of phase lock between the neurons in a local domain. Cortico-cortical, thalamic, basal ganglia, limbic, and reticular-excitatory inputs initiate phase shifts within local cortical areas. This appears to be an ongoing and continuous background process and is pervasive throughout the human central nervous system.

LORETA COHERENCE, PHASE DIFFERENCES, AND PHASE RESET

Mathematically, the computation of LORETA coherence and phase differences is the same as for the surface EEG. The difference is that the LORETA inverse solution of the location of the sources of the EEG is used to compute a time series from the center voxel of each Brodmann area. Because of the large number of voxels (e.g., 2,394), it is not possible to compute LORETA coherence and phase in real time; therefore, the selection of the center voxel as a representative voxel is commonly used (see Langer et al., 2012). This method is justified by the fact that the Laplacian operator smoothes current density in nearby voxels and the center voxel is representative of the average of the voxels that comprise a Brodmann area. We tested the relationship between currents from the center voxel of each Brodmann area and the average of the voxels that make up each Brodmann area using correlation analyses; we found that the mean correlation between the current density time series for the center voxel versus the average of voxels

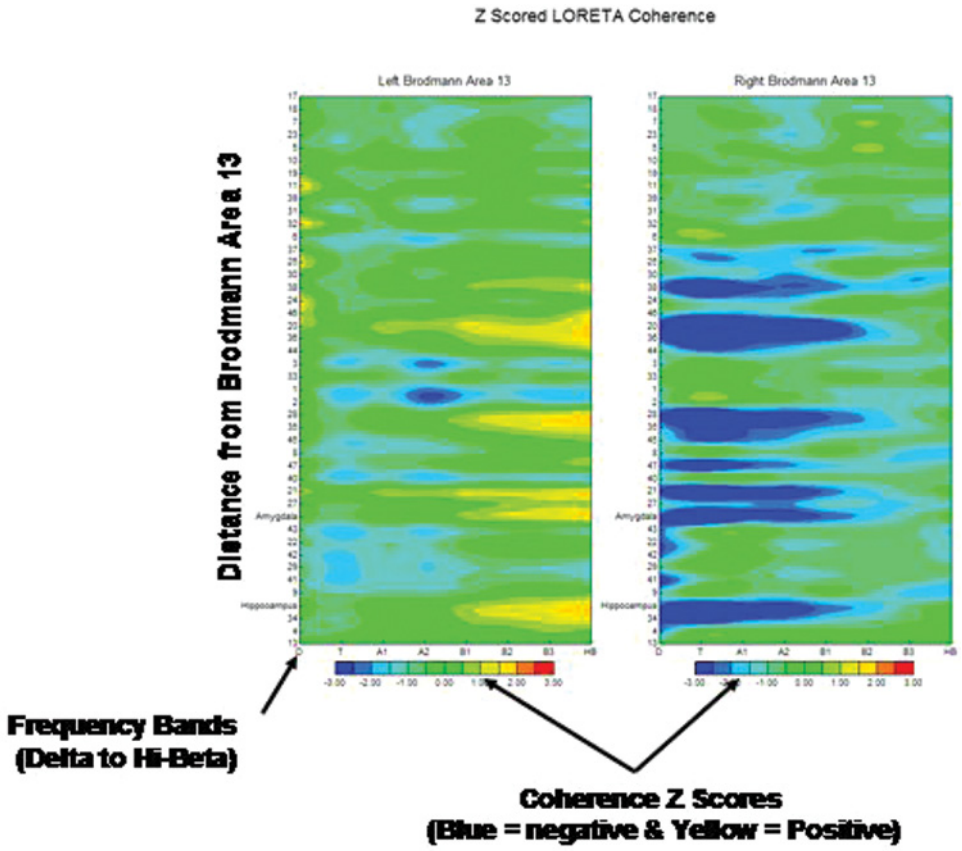

FIGURE 10. Z scores of left and right hemisphere LORETA coherence with respect to Brodmann area 13 in a right hemisphere damaged patient. *Y*-axis is the Euclidean distance with respect to Brodmann area 13. The *x*-axis is frequency bands (D = 1–4 Hz; T = 4–8 Hz; A1 = 8–10 Hz; A2 = 10–12 Hz; B1 = 12–15 Hz; B2 = 15–18 Hz; B3 = 18–25 Hz; HiB = 25–30 Hz). The colors represent the magnitude of *Z* scores with blue = negative *Z* scores and green to red the positive Z scores (±3 *SD*). This shows reduced connectivity in the right temporal lobe, amygdala and hippocampus in the lower frequency bands. The alternating horizontal bands of high and low coherence reflect the U-shaped cortico-cortical axons that connect different Brodmann areas. (Color figure available online.)

in each Brodmann area was 0.898 with a sample size of 1,792 time points and p was less than .00000000001. The center voxel is, therefore, representative of the average and is a better choice than the average of all voxels because currents from adjacent Brodmann areas will likely influence the average current density more than the center voxel current density because of the distance between the center and the boundary of adjacent Brodmann areas. Figure 10 is an example of LORETA coherence Z scores ordered as a function of distance between Brodmann area 13 and all other Brodmann areas.

SYMPTOM CHECK LIST LINKAGE BETWEEN STRUCTURE AND FUNCTION

Surface EEG

Based on these facts and other supporting science, a Symptom Check List (SCL) was developed as shown in Figure 11. The goal of the SCL is to link structure to function based on the spatial overlap of functional and clinical studies using fMRI, PET, and EEG/MEG as well as the clinical neurological science of strokes, tumors, and lesions. The SCL generates a scalp model of likely brain regions expected to be related to the patient's symptoms in the ''Hypotheses'' head. The ''Match'' head shows the EEG Z scores in the patient's record that match the hypothesized locations, and the ''Mismatch'' head shows the significant EEG measures that failed to match the hypothesized locations. It is possible that the mismatches represent ''compensatory'' processes; and, in this way, one can focus on the most likely ''weak'' brain systems linked to the patient's symptoms as discussed by Alexander Luria (1973). The ''Protocol'' on the right is a listing of measures that matched the hypothesized locations and can be saved in a file and are automatically

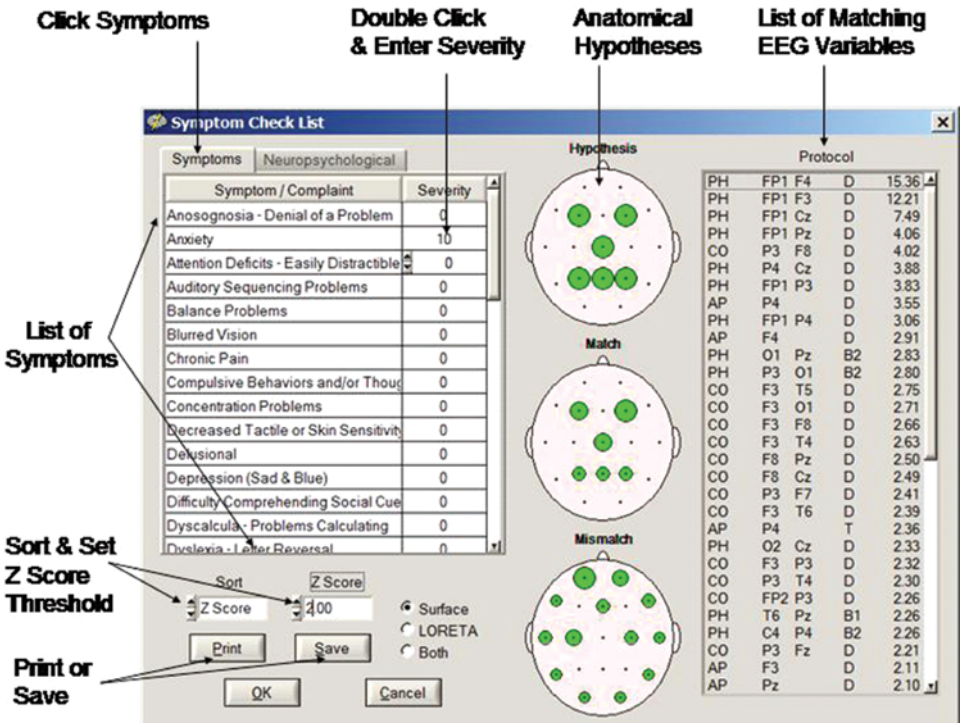

FIGURE 11. Example of an Automatic Neurofeedback Protocol generator using a Symptom Check List (SCL) where clinicians conduct a clinical interview and behavioral tests and then perform a qEEG. The SCL uses the qEEG results and the symptom or diagnosis selected by the clinician to match deviant qEEG locations to the symptoms. The qEEG results are categorized into two groups: (a) Match of qEEG assessment to networks related to symptoms, and (b) Mismatch of the qEEG results, which are likely compensatory. One can override the selections and manually add or remove frequencies and locations. (Color figure available online.)

available to perform EEG biofeedback. The second screen is the SCL panel with ''Neuropsychological Diagnoses'' selected.

Loreta

The same scientific literature review of the fMRI, PET, and EEG/MEG literature that links symptoms and neuropsychological diagnoses to functional specialization in the brain was used to provide a linkage to the three-dimensional sources of the scalp EEG. We use Low Resolution Electromagnetic Tomographic Analysis, or ''LORETA,'' that has a 7 mm cubic spatial resolution and adequately measures all of the Brodmann areas as evidenced by 795 peer-reviewed journal articles (these articles can be found at http://www.appliedneuroscience.com/LORETA%20publications.pdf).

Similar to the surface EEG SCL, the LORETA SCL generates a list of Brodmann areas likely to be related to the patient's symptoms in the ''Hypotheses'' in the lower right list. The ''Match'' list shows the statistically significant Brodmann areas in the patient's record that match the hypothesized locations, and the ''Mismatch'' shows the Brodmann areas that failed to match the hypothesized locations. It is possible that the mismatches represent ''compensatory'' processes; in this way, one can focus on the most likely ''weak'' brain systems linked to the patient's symptoms as discussed by Alexander Luria (1973). Figure 11 is an example of the SCL panel with the ''Symptoms'' selected and the Brodmann areas selected based on the match of symptoms and regions of the brain. Figure 12 is the SCL panel with ''Neuropsychological Diagnoses'' selected.

Figure 13 is an example of changes in Brodmann area EEG across sessions when using LORETA *Z*-score neurofeedback. Reinforcement toward increased stability and homeostasis is achieved by reinforcing movement toward $Z = 0$, which is the statistical center of a group of age-matched healthy individuals who had no history of neurological or psychological disorders. No individual achieves exactly $Z = 0$; however, the set point of a homeostatic statistic oscillates around $Z = 0$ and helps reduce dysregulation in hubs and modules linked to the patient's symptoms.

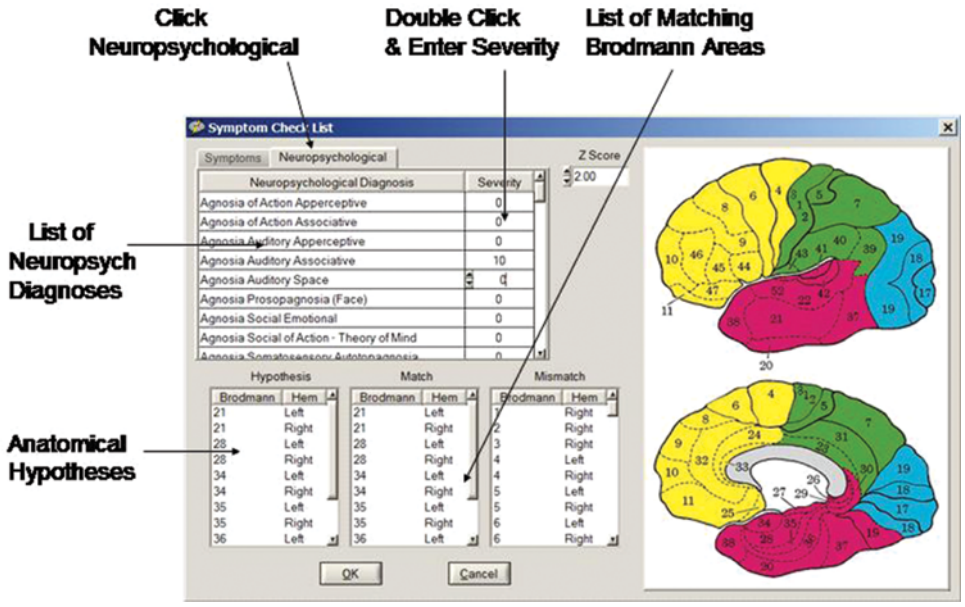

FIGURE 12. Example of an Automatic Neurofeedback Protocol generator using a Symptom Check List (SCL) where clinicians conduct a clinical interview and behavioral tests and then perform a qEEG. The LORETA SCL uses the qEEG results and the symptom or diagnosis selected by the clinician to match deviant qEEG Brodmann areas and Hubs to the symptoms. The LORETA assessment results are categorized into two groups: (a) Match of LORETA assessment to networks related to symptoms, and (b) Mismatch of the LORETA results, which are likely compensatory. One can override the selections and manually add or remove frequencies and locations. (Color figure available online.)

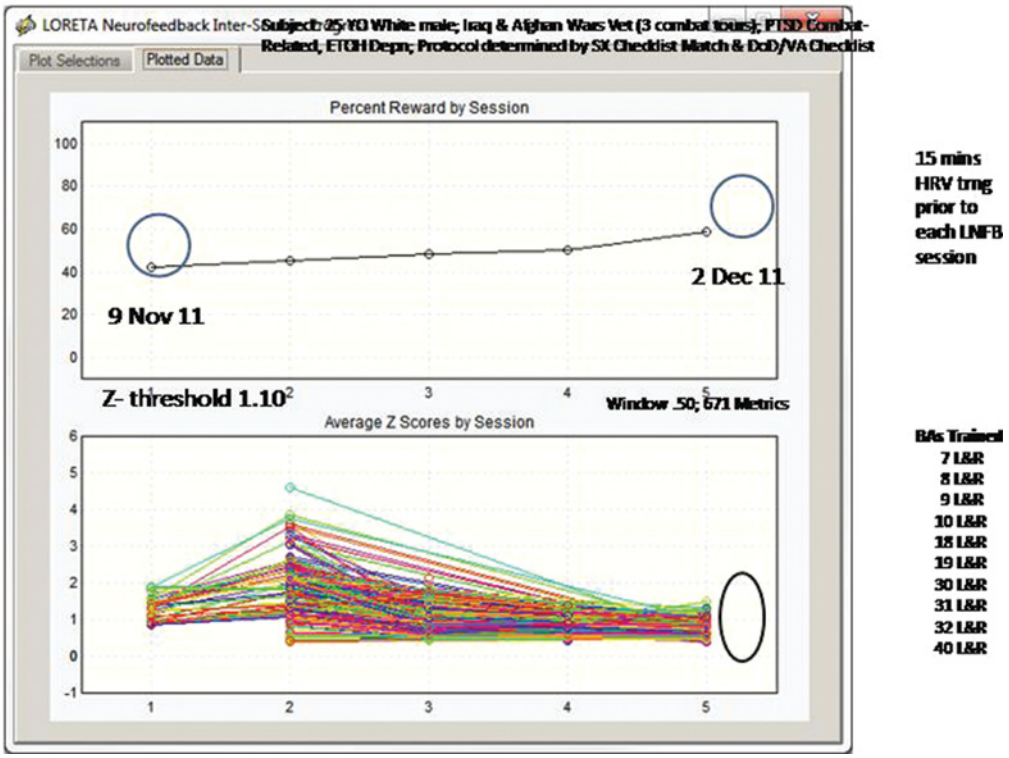

FIGURE 13. Example of movement of Brodmann area EEG toward $Z = 0$ over sessions. (From NeuroGuide version 2.7.4) (Color figure available online.)

CONCLUSIONS

Z-score neurofeedback represents a significant advancement in the field of EEG biofeedback as well as an advancement in EEG and brain science in general. *Z*-score neurofeedback allows practitioners to focus on multiple variables (e.g., absolute power, coherence, phase, etc.) while providing standardization by real-time comparisons to an age-matched group of healthy individuals. *Z*-score neurofeedback reduces guessing about whether to reinforce or inhibit a given amplitude or frequency by providing a normative database guide where one reinforces toward $Z = 0$. Normal subjects are never exactly at $Z = 0$; however, they homeostatically oscillate around $Z = 0$ and rarely exhibit consistently deviant scores that are many standard deviations from normal. Outliers and extreme *Z* scores in a patient (assuming no artifact and a valid amplifier) are indicators that can facilitate linking symptoms to networks in the brain. Another advantage of *Z*-score biofeedback is that one does not need to inhibit one frequency while reinforcing a different frequency because reinforcement toward $Z = 0$ accomplishes both at the same time. For example, a patient with elevated theta and reduced beta frequency amplitude does not require a separate inhibit setting because movement toward $Z = 0$ simultaneously normalizes elevated and low amplitude events. Also, *Z*-score biofeedback provides automatic artifact rejection because artifact creates large *Z* scores and only *Z* scores approaching $Z = 0$ are reinforced. Finally, LORETA *Z*-score biofeedback efficiently targets hubs and modules in the brain known to be related to symptoms and clinical disorders. Avoiding compensatory systems while targeting three-dimensional brain regions linked to symptoms holds the promise of better clinical outcome in fewer sessions. LORETA neurofeedback has already been shown to match the efficacy of functional MRI neurofeedback, but at a fraction of the cost of a 50-ton, $3 million MRI magnet with costs of $40,000 per month

for liquid helium. Trends in the neuroscience of EEG biofeedback paint a bright future in psychology and psychiatry and EEG neurofeedback when it adheres to the principles of operant conditioning. This trend will continue to grow and touch the lives of many more patients in the future (Thatcher, 2011, 2012).

REFERENCES

Applied Neuroscience. (n.d.). What our clients say about NeuroGuide NeuroFeedback . . . . Retrieved from http://www.appliedneuroscience.com/TestimonialNF.htm

Arns, M., de Ridder, S., Strehl, U., Breteler, M., & Coenen, A. (2009). Efficacy of neurofeedback treatment in ADHD: The effects on inattention, impulsivity and hyperactivity: A meta-analysis. *Clinical EEG & Neuroscience*, *40*, 180–189.

Balleine, B. W., & Dickinson, A. (1998). Goal-directed instrumental action: Contingency and incentive learning and their cortical substrates. *Neuropharmacology*, *37*, 407–419.

Balleine, B. W., Liljeholm, M., & Ostlund, S. B. (2009). The integrative function of the basal ganglia in instrumental conditioning. *Behavior & Brain Research*, *199*, 43–52.

Balleine, B. W., & Ostlund, S. B. (2007). Still at the choice-point: Action selection and initiation in instrumental conditioning. *Annals of the New York Academy of Sciences*, *1104*, 147–171.

Breakspear, M., & Williams, L. M. (2004). A novel method for the topographic analysis of neural activity reveals formation and dissolution of 'dynamic cell assemblies.' *Journal of Computational Neuroscience*, *16*, 49–68.

Buzsaki, G. (2006). *Rhythms of the brain*. New York, NY: Oxford University.

Clark, D. L., Boutros, N. N., & Mendez, M. F. (2010). *The brain and behavior: An introduction to behavioral neuroanatomy*. Cambridge, England: Cambridge University Press.

Collura, T. F., Guan, J., Tarrant, J., Bailey, J., & Starr, F. (2010). EEG biofeedback case studies using live Z-score training and a normative database. *Journal of Neurotherapy*, *14*, 22–46.

Cooper, R., Winter, A. L., Crow, H. J., & Walter, W. G. (1965). Comparison of subcortical, cortical, and scalp activity using chronically indwelling electrodes in man. *Electroencephalography & Clinical Neurophysiology*, *18*, 217–228.

Ermentrout, G. B., Galán, R. F., & Urban, N. N. (2007). Reliability, synchrony and noise. *Trends in Neuroscience*, *31*, 428–434.

Freeman, W. J., Burke, B. C., & Homes, M. D. (2003). A periodic phase re-setting in scalp EEG of beta-gamma oscillations by state transitions at alpha-theta rates. *Human Brain Mapping*, *19*, 248–272.

Freeman, W. J., Homes, M. D., West, G. A., & Vanhatlo, S. (2006). Fine spatiotemporal structure of phase in human intracranial EEG. *Clinical Neurophysiology*, *117*, 1228–1243.

Freeman, W. J., & Rogers, L. J. (2002). Fine temporal resolution of analytic phase reveals episodic synchronization by state transitions in gamma EEGs. *Journal of Neurophysiology*, *87*, 937–945.

Galán, R. F., Ermentrout, G. B., & Urban, N. N. (2005). Efficient estimation of phase-resetting curves in real neurons and its significance for neural-network modeling. *Physical Review Letters*, *94*, 188–164.

GoCognitive. (n.d.-a). Neurofeedback in psychiatric disorder [Video file]. Retrieved from http://www.gocognitive.net/interviews/neurofeedback-psychiatric-disorders

GoCognitive. (n.d.-b). The specificity of feedback [Video file]. Retrieved from http://www.gocognitive.net/interviews/specificity-feedback

Granger, C. W. J., & Hatanka, M. (1964). *Spectral analysis of economic time series*. Princeton, NJ: Princeton University Press.

Gray, C. M., Konig, P., Engel, A. K., & Singer, W. (1989). Oscillatory responses in cat visual cortex exhibit intercolumnar synchronization which reflects global stimulus properties. *Nature*, *338*, 334–340.

Hagmann, P., Cammoun, L., Gigandet, X., Meuli, R., Honey, C. J., Wedeen, V. J., & Sporns, O. (2008). Mapping the structural core of human cerebral cortex. *PLoS Biology*, *6*, e159.

Hammer, B. U., Colbert, A. P., Brown, K. A., & Ilioi, E. C. (2011). Neurofeedback for insomnia: A pilot study of Z-score SMR and individualized protocols. *Applied Psychophysiology & Biofeedback*, *36*, 251–264.

Hughes, S. W., & Crunelli, V. (2007). Just a phase they're going through: The complex interaction of intrinsic high-threshold bursting and gap junctions in the generation of thalamic α and θ rhythms. *International Journal of Psychophysiology*, *64*, 3–17.

John, E. R. (2005). From synchronous neural discharges to subjective awareness? *Progress in Brain Research*, *150*, 143–171.

John, E. R., Prichep, L. S., & Easton, P. (1987). Normative data banks and neurometrics: Basic concepts, methods and results of norm construction. In A. Remond (Ed.), *Handbook of electroencephalography and clinical neurophysiology: Vol. III: Computer analysis of the EEG and other neurophysiological signals* (pp. 449–495). Amsterdam, The Netherlands: Elsevier.

Kandel, E. R. (2006). *In search of memory*. New York, NY: Norton.

Lachaux, J.-P., Rodriguez, E., Le Van Quyen, M., Lutz, A., Martinerie, J., & Varela, F. J. (2000). Studying single-trials of phase synchronous activity in the brain. *International Journal of Bifurcation Chaos*, *10*, 2429–2439.

Lachaux, J.-P., Rodriguez, E., Martinerie, J., & Varela, F. J. (1999). Measuring phase locking in brain signals. *Human Brain Mapping*, *8*, 194–208.

Lancaster, J. L., Woldorff, M. G., Parsons, L. M., Liotti, M., Freitas, C. S., & Rainey, L. (2000). Automatic Talairach atlas labels for functional brain mapping. *Human Brain Mapping*, *10*, 120–131.

Langer, N., Pedroni, A., Gianotti, L. R., Hanggi, J., Knoch, D., & Jancke, L. (2012). Functional brain network efficiency predicts intelligence. *Human Brain Mapping*, *33*, 1393–1406.

Le Van Quyen, M., Foucher, J., Lachaux, J.-P., Rodriguez, E., Lutz, A., Martinerie, J., & Varela, F. J. (2001). Comparison of Hilbert transform and wavelet methods for the analysis of neuronal locking. *Journal of Neuroscience Methods*, *111*, 83–89.

Lopes da Silva, F. H. (1995). Dynamic of electrical activity of the brain, networks, and modulating systems. In P. Nunez (Ed.), *Neocortical dynamics and human EEG rhythms* (pp. 249–271). New York, NY: Oxford University Press.

Luria, A. (1973). *The working brain: An introduction to neuropsychology*. Baltimore, MD: Penguin.

Mesulam, M. M. (2000). *Principles of behavioral and cognitive neurology* (2nd Ed.). New York, NY: Oxford University Press.

Montez, T., Linkenkaer-Hansen, K., Van Dijk, B. W., & Stam, C. J. (2006). Synchronization likelihood with explicit time-frequency priors. *Neuroimage*, *33*, 1117–1125.

Nargeot, R., Baxter, D. A., & Byrne, J. M. (1999). *In vitro* analog of operant conditioning in *aplysia*, I: Contingent reinforcement modifies the functional dynamics of an identified neuron. *Journal of Neuroscience*, *19*, 2247–2260.

Nargeot, R. D., Baxter, A., Patterson, G. W., & Byrne, J. H. (1999). Dopaminergic synapses mediate neuronal changes in an analogue of operant conditioning. *Journal of Neurophysiology*, *81*, 1983–1987.

Nunez, P. (1981). *Electrical fields of the brain*. New York, NY: Oxford University Press.

Nunez, P. L. (1995). *Neocortical dynamics and human EEG rhythms*. New York, NY: Oxford University Press.

Otnes, R. K., & Enochson, L. (1978). *Applied time series analysis*. New York, NY: Wiley.

Pascual-Marqui, R. D., Michel, C. M., & Lehmann, D. (1994). Low resolution electromagnetic tomography: A new method for localizing electrical activity in the brain. *International Journal of Psychophysiology*, *18*, 49–65.

Pikovsky, A., Rosenblum, M., & Kurths, J. (2003). *Synchronization: A universal concept in nonlinear sciences*. New York, NY: Cambridge University Press.

Rabinovich, M. I., Afraimovich, V. S., Christian, B., & Varona, P. (2012). Information flow

dynamics in the brain. *Physics of Life Reviews*, *9*, 51–73.

Rudrauf, R., Cosmelli, D., Chavez, A., Renault, B., Marttinerie, J., & Le Van Quyen, M. (2006). Frequency flows and the time-frequency dynamics of multivariate phase synchronization in brain signals. *Neuroimage*, *31*, 209–227.

Schultz, W. (2006). Behavioral theories and the neurophysiology of reward. *Annual Review of Psychology*, *57*, 87–115.

Sherlin, L. H., Arns, M., Lubar, J., Heinrich, H., Kerson, C., Strehl, U., & Sterman, M. B. (2011). Neurofeedback and basic learning theory: Implications for research and practice. *Journal of Neurotherapy*, *15*, 292–304.

Smeal, R. M., Ermentrout, G. B., & White, J. A. (2010). Phase-response curves and synchronized neural networks. *Philosophical Transactions of the Royal Society of London Biological Sciences*, *365*, 2407–2422.

Stam, C. J., & Van Dijk, B. W. (2002). Synchronization likelihood: An unbiased measure of generalized synchronization in multivariate data sets. *Physica D*, *163*, 236–241.

Stam, C. J., & van Straaten, E. C. W. (2012). The organization of physiological brain networks. *Clinical Neurophysiology*, *123*, 1067–1087. doi: 10.1016/j.clinph.2012.01.011

Tass, P. A. (2007). *Phase resetting in medicine and biology*. Berlin, Germany: Springer-Verlag.

Thatcher, R. W. (1998). EEG normative databases and EEG biofeedback. *Journal of Neurotherapy*, *2*(4), 8–39.

Thatcher, R. W. (1999). EEG database guided neurotherapy. In J. R. Evans & A. Abarbanel (Eds.), *Introduction to quantitative EEG and neurofeedback* (pp. 23–61). San Diego, CA: Academic Press.

Thatcher, R. W. (2000a, September). *An EEG least action model of biofeedback*. Paper presented at the 8th Annual ISNR conference, St. Paul, MN.

Thatcher, R. W. (2000b). EEG operant conditioning (biofeedback) and traumatic brain injury. *Clinical Electroencephalography*, *31*, 38–44.

Thatcher, R. W. (2011). Neuropsychiatry and quantitative electroencephalography in the 21st century. *Neuropsychiatry*, *1*, 495–514. doi: 10.2217/npv.11

Thatcher, R. W. (2012). *Handbook of quantitative electroencephalography and EEG biofeedback*. Petersburg, FL: Anipublishing.

Thatcher, R. W., & Lubar, J. F. (2008). History of the scientific standards of QEEG normative databases. In T. Budzynski, H. Budzynski, J. Evans, & A. Abarbanel (Eds.), *Introduction to QEEG and neurofeedback: Advanced theory and applications* (pp. 36–55). San Diego, CA: Academic Press.

Thatcher, R. W., North, D., & Biver, C. (2005). Evaluation and validity of a LORETA normative EEG database. *Clinical EEG & Neuroscience*, *36*, 116–122.

Thatcher, R. W., North, D., & Biver, C. (2008a). Development of cortical connectivity as measured by EEG coherence and phase. *Human Brain Mapping*, *29*, 1400–1415.

Thatcher, R. W., North, D., & Biver, C. (2008b). Intelligence and EEG phase reset: A two-compartmental model of phase shift and lock. *NeuroImage*, *42*, 1639–1653.

Thatcher, R. W., North, D., & Biver, C. (2009). Self organized criticality and the development of EEG phase reset. *Human Brain Mapping*, *30*, 553–574.

Thatcher, R. W., North, D. M., & Biver, C. J. (2012). Diffusion tensor imaging modules correlated with LORETA electrical neuroimaging modules. *Human Brain Mapping*, *33*, 1062–1075.

Thatcher, R. W., North, D., Neurbrander, J., Biver, C. J., Cutler, S. & DeFina, P. (2009). Autism and EEG phase reset: Deficient GABA mediated inhibition in thalamocortical circuits. *Developmental Neuropsychology*, *34*, 780–800.

Thatcher, R. W., Walker, R. A., Biver, C., North, D., & Curtin, R. (2003). Quantitative EEG normative databases: Validation and clinical correlation. *Journal of Neurotherapy*, *7*, 87–122.

Tiesinga, P. H., & Sejnowski, T. J. (2010). Mechanisms for phase shifting in cortical networks and their role in communication

through coherence. *Frontiers in Human Neuroscience*, *4*(196), 1–14.

Tonkonogy, J. M., & Puente, A. E. (2009). *Localization of clinical syndromes in neuropsychology and neuroscience*. New York, NY: Springer.

Varela, F. J. (1995). Resonant cell assemblies: A new approach to cognitive functions and neuronal locking. *Biological Research*, *28*, 81–95.

Varela, F., Lachaux, J. P., Rodriguez, E., & Martinerie, J. (2001). The brainweb: Phase-synchronization and large scale integration. *Nature Reviews Neuroscience*, *2*, 229–239.

Wang, X. J. (2002). Pacemaker neurons for the theta rhythm and their synchronization in the septohippocampal reciprocal loop. *Journal of Neurophysiology*, *87*, 889–900.

Wangler, S., Gevensleben, H., Albrecht, B., Studer, P., Rothenberger, A., Moll, G. H., & Heinrich, H. (2011). Neurofeedback in children with ADHD: Specific event-related potential findings of a randomized controlled trial. *Clinical Neurophysiology*, *122*, 942–950.